Cumulant Analysis of Charge Recombination Kinetics in Bacterial Reaction Centers Reconstituted into Lipid Vesicles

Gerardo Palazzo,* Antonia Mallardi,† Mauro Giustini,‡ Debora Berti,§ and Giovanni Venturoli¶
*Dip. Chimica, Università di Bari, I-70126 Bari; †CS-CFILM (CNR), Bari; ‡Dip. Chimica, Università "La Sapienza," Roma; §CSGI-Dip. Chimica, Università di Firenze, Firenze; ¶Lab. Biochimica Biofisica, Dip. Biologia, Università di Bologna, Bologna, Italy

ABSTRACT The kinetics of charge recombination between the primary photoxidized donor (P^+) and the secondary reduced quinone acceptor (Q_B^-) have been studied in reaction centers (RCs) from the purple photosynthetic bacterium *Rhodobacter sphaeroides* incorporated into lecithin vesicles containing large ubiquinone pools over the temperature range 275 K $\leq$ T $\leq$ 307 K. To account for the non-exponential kinetics of P^+ re-reduction observed following a flash, a new approach has been developed, based on the following assumptions: 1) the exchange of quinone between different vesicles is negligible; 2) the exchange of quinone between the Q_B site of the RC and the quinone pool within each single vesicle is faster than the return of the electron from the primary reduced acceptor Q_A^- to P^+; 3) the size polydispersity of proteoliposomes and the distribution of quinone molecules among them result in a quinone concentration distribution function, P(Q). The first and second moments of P(Q) have been evaluated from the size distribution of proteoliposomes probed by quasi-elastic light scattering (mean radius, $\langle R \rangle$ = (50 $\pm$ 15) nm). Following these premises, we describe the kinetics of $P^+Q_B^-$ recombination with a truncated cumulant expansion and relate it to P(Q) and to the free energy changes for $Q_A^-Q_B \rightarrow Q_AQ_B^-$ electron transfer (ΔG°_{AB}) and for quinone binding (ΔG°_{bind}) at Q_B. The model accounts well for the temperature and quinone dependence of the charge recombination kinetics, yielding $\Delta G^\circ_{AB} = -7.67 \pm 0.05$ kJ mol^{-1} and $\Delta G^\circ_{bind} = -14.6 \pm 0.6$ kJ mol^{-1} at 298 K.

INTRODUCTION

In bacterial photosynthesis the primary events of energy transduction are accomplished by the reaction center (RC), an integral pigment-protein complex spanning the intracytoplasmic membrane and promoting light-induced charge separation across the membrane dielectric (Gunner, 1991). In the RC of the purple bacterium *Rhodobacter sphaeroides*, photon energy promotes the primary electron donor, a bacteriochlorophyll dimer (P), to the first excited singlet state (P*). An electron is consequently transferred (via bacteriopheophytin) from P* to a first ubiquinone-10 (UQ_{10}) electron acceptor (Q_A), generating the primary charge separated state $P^+Q_A^-$. The electron present on Q_A is then delivered to a secondary quinone acceptor, Q_B. In the absence of an electron donor to P^+ the electron on Q_B^- recombines with the hole on P^+ (Feher et al., 1989).

In the presence of electron donors to P^+, a second photoactivation of the RC leads to the double reduction and protonation of Q_B, which leaves the RC in its quinol state, UQH_2 (Wraight, 1981; McPherson et al., 1990). In vivo, the function of the acceptor quinone complex is to deliver reducing equivalents to a pool of ubiquinone molecules present in the native membrane in stoichiometric excess over the RC (Crofts and Wraight, 1983). This occurs through the free exchange of UQH_2, at the Q_B site of the RC, with oxidized quinone from the pool. In view of the detailed functional and structural information gained in the last decades, the quinone acceptor system of bacterial RCs has become a reference model in the study of the diverse interactions of quinones with electron transfer complexes (Cramer and Knaff, 1990).

A very convenient way of studying the functional properties of the acceptor quinone complex is through the kinetics of charge recombination from either the $P^+Q_B^-$ state or the $P^+Q_A^-$ state, when in the presence of inhibitors of the Q_A^- to Q_B electron transfer. These reactions have been extensively studied, yielding to a wealth of information on the energetics of the electron transfer and protonation events involving the quinone acceptor complex (Mancino et al., 1984; Kleinfeld et al., 1984a; Kleinfeld et al., 1985; Gao et al., 1991). Moreover, with the availability of the X-ray diffraction structures of RCs from *R. sphaeroides* (Allen et al., 1987a, 1987b; Ermler et al., 1994) and *Rhodopseudomonas viridis* (Deisenhofer et al., 1984, 1985), the analysis of charge recombination kinetics within these RCs has been a valuable tool in testing electron transfer theories and in investigating the protein dynamics associated with charge transfer events (Gunner et al., 1986, 1996; Feher et al., 1988; Labahn et al., 1995; Ortega et al., 1996; McMahon et al., 1998).

These studies have been mainly performed in detergent RC micelles; only in a few cases charge recombination has been examined in RCs reincorporated into artificial phospholipid vesicles more closely mimicking their native environment (Wraight, 1981; Baciou et al., 1990; Agostiano et al., 1995; Nagy et al., 1999). When RCs are inserted into UQ-enriched liposomes, the kinetics of $P^+Q_B^-$ recombination is expected to carry information on the exchange interactions of ubiquinone between the RC and the membrane pool (Shinkarev and Wraight, 1993). In spite of this possi-

Received for publication 16 February 2000 and in final form 14 June 2000.
Address reprint requests to Dr. Gerardo Palazzo, Universita di Bari, Dip. Chimica, via Orabona 4, 1-70126 Bari, Italy. Tel.: 39-080-5442011; Fax: 39-080-5442129; E-mail: palazzo@chimica.uniba.it.

0006-3495/00/09/1171/09 $2.00

bility, no systematic study has been carried out in proteoliposomes on the effect of quinone concentration in the lipid phase.

In the present paper the kinetics of $P^+Q_B^-$ charge recombination have been studied in RCs from *R. sphaeroides* reconstituted into lecithin vesicles in the presence of large UQ_{10} pools and over a range of temperatures. We show that the observed non-exponential kinetics of P^+ relaxation following a short flash of light can be satisfactorily described by assuming a fast exchange of quinone at the Q_B site of the RC and by considering a rate distribution function arising from an heterogeneity in UQ_{10} concentration within the vesicle population.

MATERIALS AND METHODS

Except where otherwise stated, all chemicals were from Sigma Chemical Co. (Darmstadt, Germany), of the highest purity and used without further purification.

The RCs were isolated and purified from *R. sphaeroides* R-26 according to Gray et al. (1990). The RC containing vesicles were prepared as follows. Soybean phosphatidylcholine (PC) (Epikuron 200, generous gift of Lukas Meyer, Germany) and the proper amount of ubiquinone-10 were dissolved in chloroform, dried under N_2 and resuspended in 10 mM imidazole/100 mM KCl/3% Na cholate (pH 7) buffer. RCs (in 10 mM Tris-HCl, 0.025% lauryldimethylamine *N*-oxide (LDAO), 1 mM EDTA, pH 7) were added to this suspension, previously sonicated until clarity. Detergent removal was obtained by eluting this suspension through a Sephadex G-50 (Pharmacia, Sweden) column with 10 mM imidazole/100 mM KCl (pH 7) buffer. Detergent removal results in RC-containing small unilamellar vesicles (SUVs) (Venturoli et al., 1993). The mole ratio PC/RC was fixed at 1000 and the RC concentration was about 5 μM.

The kinetics of charge recombination were measured spectrophotometrically by following the re-reduction of P^+ generated by a short (3 μs half-duration) xenon flash at 540 nm and at 605 nm (Feher and Okamura, 1978). Flash-induced absorption changes (ΔAbs) were recorded also at 450 nm, a wavelength which includes contributions from both P^+ and semiquinone formation on the acceptor complex (Feher and Okamura, 1978). Flash-kinetic spectrophotometry was performed by using an apparatus of local design (Mallardi et al., 1997).

Sizing of the SUVs was performed by means of quasi-elastic light scattering (QELS) with the instrumental setup described in Berti et al. (1999). Basically the normalized temporal autocorrelation function $g_2(q, \tau)$ of the intensity of the light scattered by the sample at an angle θ with respect to the incident beam has been obtained. This quantity is related to the intensity of the scattered electric field $g_1(q, \tau)$ through $g_2(q, \tau) = 1 + \beta|g_1(q, \tau)|^2$, where $q = (4\pi n/\lambda)\sin(\theta/2)$ (λ being the wavelength of the beam and n the refractive index of the medium) and β is an instrumental parameter connected to the signal-to-noise ratio (Corti, 1985; Chu, 1991). In a solution of monodisperse spherical vesicles, when q^{-1} is much larger than the mean intraparticle distance, the autocorrelation function of the scattered electric field decays through a diffusive mechanism and $g_2(q, \tau) = 1 + \beta \exp(-2D_C q^2 \tau)$, where D_C is the collective diffusion coefficient of the particles. In the infinite dilution limit, the radius R of the particle can be evaluated from D_C by means of the Stokes-Einstein relationship, $D_C = k_B T/6\pi\eta_0 R$, where η_0 is the solvent viscosity (Corti, 1985).

All the numerical fitting procedures were performed running the STEFIT software (STELAR, Italy) and using routinely three different algorithms (simplex, Powell, quadric) in order to avoid local minima in χ^2 minimization. Unless otherwise stated, confidence limits (67%) were evaluated as linear joint confidence intervals.

RESULTS AND DISCUSSION

Kinetics of P^+ dark relaxation and quinone binding equilibria

In *R. sphaeroides* RCs, electron transfer reactions following absorption of a photon can be conveniently described by the following scheme (Shinkarev and Wraight, 1993):

$$PQ_AQ_B \underset{k_{AP}}{\overset{h\nu}{\rightleftharpoons}} P^+Q_A^-Q_B \overset{L_{AB}}{\longleftrightarrow} P^+Q_AQ_B^- \qquad (1)$$

$$k_{QB}^* \uparrow\downarrow k_{BQ}^* \qquad k_{QB} \uparrow\downarrow k_{BQ}$$

$$PQ_A + Q \underset{k_{AP}}{\overset{h\nu}{\rightleftharpoons}} P^+Q_A^- + Q$$

where k_{QB} (k_{QB}^*) and k_{BQ} (k_{BQ}^*) are the second-order and first-order rate constants for UQ_{10} binding and release, respectively, after (before) the light absorption and L_{AB} is the constant for $Q_A^-Q_B \rightarrow Q_AQ_B^-$ equilibrium, which is much faster than $P^+Q_A^- \rightarrow P\ Q_A$ recombination ($k_{AP}^{-1} \approx 0.1$ s) (Vermeglio and Clayton, 1977; Kleinfeld et al., 1984a). Ubiquinone is tightly bound to the protein at the Q_A site, acting as a prosthetic group, while Q_B, in the oxidized form, can freely exchange with a UQ_{10} pool present in the membrane bilayer. At room temperature, following photoactivation, the electron returns from Q_B^- to P^+ via the primary quinone acceptor Q_A, the contribution of direct tunneling being negligible (Kleinfeld et al., 1984a).

Under pseudo-first-order conditions, i.e., in the presence of a stoichiometric excess of UQ_{10} over the RC, Scheme 1 can be analytically solved (Shinkarev and Wraight, 1993). On this basis, the decay of P^+ following a flash is described by a biexponential function, i.e.:

$$l(t) = P^+(t)/P^+(0) = Fe^{-k_F t} + Se^{-k_S t} \qquad (2)$$

where k_F and k_S are given by:

$$k_F + k_S = \frac{k_{AP} + k_{BQ}}{1 + L_{AB}} + k_{QB}Q + k_{AP} \qquad (3)$$

$$k_F k_S = \frac{k_{AP}^2 + k_{BQ}k_{AP} + k_{AP}k_{QB}Q}{1 + L_{AB}} \qquad (4)$$

In Eqs. 2–4, Q is the quinone concentration in the membrane pool, F and S = 1 − F are the fraction of the fast and slow components which depend in general upon Q.

When the exchange of quinone between the RC and the exogenous pool is slower than $P^+Q_A^-$ recombination, $k_F = k_{AP}$ and F is simply the fraction of RCs without Q_B at the time of the flash. If, on the contrary, quinone exchange at Q_B is faster than the return of the electron from Q_A^- to P^+, as discussed in detail by Shinkarev and Wraight (1993), the expected kinetics of P^+ re-reduction are well approximated by a monoexponential decay, characterized by a rate con-

stant (k_P) that decreases as Q is increased, according to:

$$k_P = k_{AP}\left(1 + \frac{L_{AB}K_{bind}Q}{1 + K_{bind}Q}\right)^{-1} \quad (5)$$

where $K_{bind} = k_{QB}/k_{BQ}$ represents the equilibrium constant for UQ_{10} binding after the light absorption.

We have analyzed the kinetics of charge recombination in *R. sphaeroides* RCs reconstituted into liposomes in the presence of a large UQ_{10} pool, at two UQ/RC stoichiometric ratios, over the temperature range 275 K $\leq$ T $\leq$ 307 K. Examples of the kinetics of the absorbance change (ΔAbs) recorded at 450, 540, and 605 nm following a flash are shown in Fig. 1 for UQ_{10}/RC = 10 at T = 304 K. As is evident in Fig. 1, and under all conditions tested, the experimental P^+ decay following a flash does not fit monoexponential kinetics; in a first attempt, therefore, the experimental kinetics, $l(t) = \Delta Abs(t)/\Delta Abs(0)$, have been fitted to a double exponential function (Eq. 2). Since at each temperature and UQ_{10}/RC ratios tested the decay kinetics recorded at the three different wavelengths were found in excellent agreement when properly normalized, a procedure of global analysis was adopted (Becheem, 1992) in order to increase the confidence in the fitting parameters. Nonlinear χ^2 minimization performed simultaneously on the kinetics recorded at 450, 540, and 605 nm yields the parameters listed in Table 1. A deconvolution of the $P^+Q_B^-$ charge recombination kinetics in two exponential components characterized by rate constants compatible with the results of Table 1 has been reported for RCs reconstituted into liposomes in the presence of excess quinone (Agostiano et al., 1995).

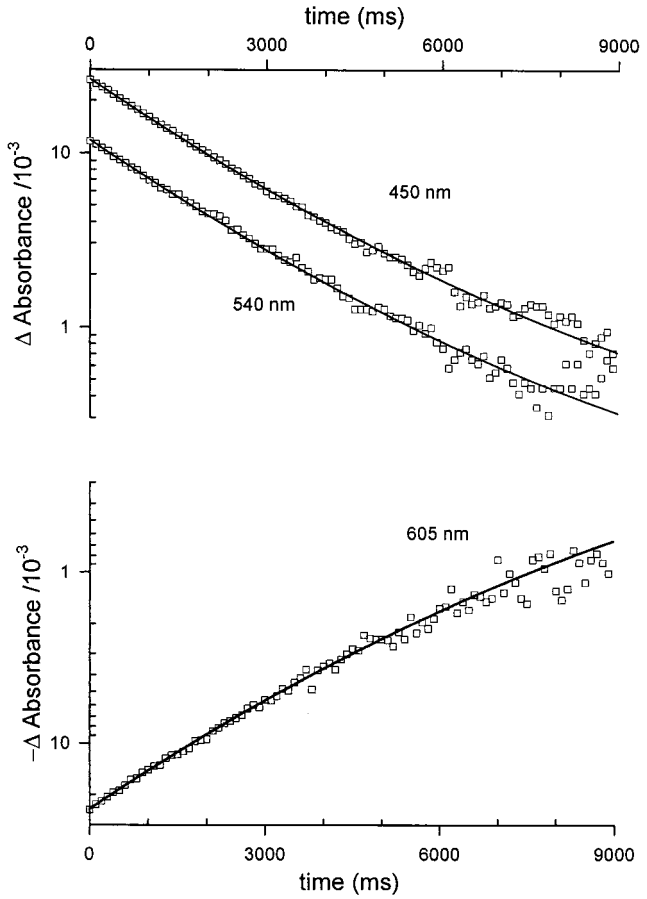

FIGURE 1 Kinetics of charge recombination following a flash of light measured at 450, 540, and 605 nm in *R. sphaeroides* RC incorporated into lecithin vesicles containing a pool of ubiquinone ([Q]/[RC] = 10). Proteoliposomes corresponding to a final RC concentration of 5 μM were suspended in 10 mM imidazole/100 mM KCl (pH 7) buffer. Each trace is the average of 4 measurements performed at 304 K. To increase figure readability only 10% of the experimental values digitized during the dark relaxation following the flash are plotted as open squares. All information has been used in numerical fitting. Continuous lines show the best fit to Eq. 6 obtained by numerical χ^2 minimization performed simultaneously over traces recorded at the three wavelengths.

Although a satisfactory fit could be obtained for each experimental condition, the corresponding values of k_F and k_S appear to be physically incompatible with the expectations of Scheme 1, as shown by the following argument.

Scheme 1 predicts a biexponential decay of P^+ when quinone exchange between the pool and the Q_B site is slower than or comparable in rate with $P^+Q_A^-$ recombination. The possibility that the parameters of Table 1 reflect a slow exchange can be immediately rejected, since in this case k_F should coincide with k_{AP}, which is approx. 10 s^{-1} and is characterized by a slight inverse temperature dependence on the temperature range investigated (Feher et al., 1987). The k_F values obtained from a biexponential deconvolution of P^+ decays are at least one order of magnitude

TABLE 1 Parameters obtained from biexponential deconvolution (Eq. 2) and cumulant analysis (Eq. 6) of charge recombination kinetics

T (°C)	k_F (s^{-1}) ($\pm$ error)	k_S (s^{-1}) ($\pm$ error)	F ($\pm$ error)	$\langle k_P \rangle$ (s^{-1}) ($\pm$ error)	σ_k (s^{-1}) ($\pm$ error)
			[Q]/[RC] = 25		
2	0.37	0.17	0.47	0.25	0.08
	(0.05)	(0.02)	(0.11)	(0.01)	(0.04)
13	0.49	0.23	0.44	0.35	0.11
	(0.19)	(0.05)	(0.34)	(0.01)	(0.05)
21	0.52	0.25	0.56	0.40	0.13
	(0.09)	(0.04)	(0.19)	(0.01)	(0.04)
25	0.48	0.20	0.80	0.43	0.13
	(0.03)	(0.01)	(0.06)	(0.01)	(0.07)
34	0.65	0.32	0.61	0.53	0.17
	(0.11)	(0.05)	(0.17)	(0.01)	(0.10)
			[Q]/[RC] = 10		
4	0.33	0.22	0.49	0.27	0.05
	(0.11)	(0.02)	(0.19)	(0.01)	(0.06)
11	0.41	0.25	0.46	0.33	0.09
	(0.07)	(0.01)	(0.10)	(0.01)	(0.07)
20	0.46	0.244	0.73	0.40	0.10
	(0.07)	(0.06)	(0.14)	(0.01)	(0.05)
31	0.55	0.14	0.91	0.53	0.16
	(0.01)	(0.10)	(0.01)	(0.01)	(0.07)

smaller and they clearly increase when the temperature increases. On the other hand, when assuming that quinone exchange share the same time scale of $P^+Q_A^-$ recombination, Eqs. 3 and 4 fix a lower limit for the rate constants k_F and k_S, given by $k_F + k_S > k_{AP}$ and $k_F k_S \geq k_{AP}^2/(1 + L_{AB})$. Fig. 2 shows that the data of Table 1 are in sharp conflict with the first inequality. The data are also in conflict with the second inequality by more than one order of magnitude (Fig. 2), when L_{AB} is calculated from the enthalpy ($\Delta H^o_{AB} = -13.5$ kJ mol^{-1}) and entropy ($\Delta S^o_{AB} = -19.3$ J mol^{-1} K^{-1}) changes for $Q_A^-Q_B \leftrightarrow Q_AQ_B^-$ electron transfer determined in reverse micelles of phospholipids in *N*-hexane (Mallardi et al., 1997). In detergent RC dispersions, very similar ΔH^o_{AB} and ΔS^o_{AB} values have been obtained (Mancino et al., 1984), which are expected to hold also in SUVs. We conclude that the non-exponential character of charge recombination kinetics systematically observed in liposomes cannot be accounted for by Eqs. 2–4.

Cumulant analysis

As pointed out by Shinkarev and Wraight (1993) various estimates of the rate of quinone exchange between RC and the UQ pool in the native membrane indicate that it is much faster than $P^+Q_A^-$ recombination and suggest that also in artificial phospholipid vesicles containing *R. sphaeroides* RCs and UQ_{10}, fast quinone exchange occurs. Under these conditions a monophasic kinetics of $P^+Q_B^-$ recombination is expected, characterized by a single (Q dependent) rate constant k_P (Eq. 5). However, this prediction of Scheme 1 assumes implicitly that the quinone pool is homogeneously available to all the RCs in the lipid phase. Such an assumption is expected to be seriously inappropriate in vesicles, where the size polydispersity could determine a broad quinone concentration distribution which would result in turn, according to Eq. 5, in a k_P distribution. Therefore, we describe the kinetics of $P^+Q_B^-$ recombination with a rate constant distribution function, $P(k_P)$, according to $l(t) = \Delta Abs(t)/\Delta Abs(0) = \int P(k_P)e^{-k_P t}dk_P$. A similar approach has been adopted to account for the nonexponential kinetics of $P^+Q_A^-$ recombination in RCs cooled at cryogenic temperatures in the light (Kleinfeld et al., 1984b; McMahon et al., 1998).

In order to analyze accordingly the kinetics of charge recombination, a method based on the statistical cumulant generating function formalism is proposed, which has been successfully used in the analysis of QELS data in the last two decades. Since $l(t)$ can be thought as a sum of exponential decays, exactly as the intensity autocorrelation function measured in QELS experiments (Koppel, 1972), we describe the charge recombination kinetics with a truncated cumulant expansion:

$$\ln[l(t)] = \sum_{i=1}^{N} \frac{K_i(-t)^i}{i!},$$

where K_i are the cumulants. $K_1 = \langle k_P \rangle$ gives the first moment of $P(k_P)$ and $K_2 = \sigma_k^2$ gives the second moment around the mean (Koppel, 1972). The third and fourth cumulants can be related to higher moments of $P(k_P)$, but in the case of our kinetics they have been found so close to zero that a truncation to the second term is appropriate to satisfactorily describe the charge recombination kinetics, $l(t)$, according to:

$$\ln[l(t)] = -\langle k_P \rangle t + \tfrac{1}{2}\sigma_k^2 t^2 \qquad (6)$$

Experimental decays have been fitted to Eq. 6, again performing a global analysis in which chi-square has been minimized simultaneously on the kinetic traces acquired at the three wavelengths for each condition (T, [Q]). An example of the best fitting decays obtained by this procedure is shown in Fig. 1. Under all conditions tested, deconvolution according to Eq. 6 yields accurate descriptions of the experimental kinetics, characterized by the parameters listed in Table 1. Qualitatively, as expected from Eq. 5 and from the thermodynamic parameters governing quinone binding and $Q_A^-Q_B \leftrightarrow Q_AQ_B^-$ electron transfer (Mallardi et

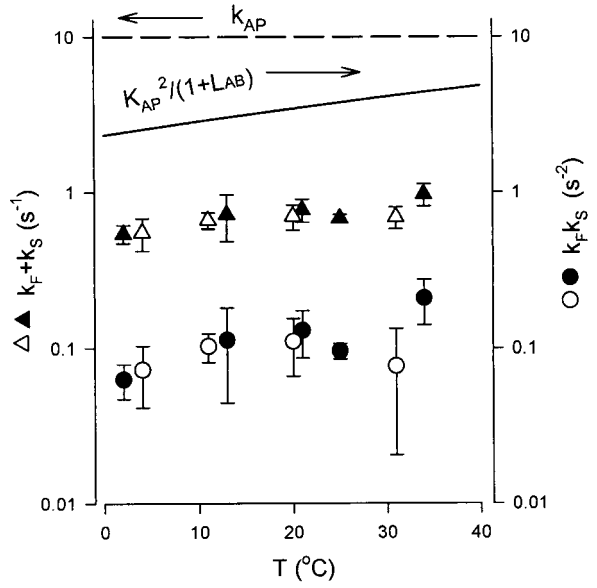

FIGURE 2 Sum (*triangles*) and product (*circles*) of the rate constants obtained from biexponential deconvolution of P^+ decay in proteoliposomes with [Q]/[RC] = 25 (*filled symbols*) and [Q]/[RC] = 10 (*open symbols*), as a function of temperature. Data are from Table 1. k_{AP} has been set equal to 10 s^{-1} (Kleinfeld et al., 1984a) and the equilibrium constant L_{AB} has been evaluated according to $L_{AB} = \exp(-\Delta H^o_{AB}/RT + \Delta S^o_{AB}/R)$, assuming for the enthalpy (ΔH^o_{AB}) and entropy (ΔS^o_{AB}) changes the values (Table 2) determined in reverse micelles (Mallardi et al., 1997). The arrows indicate the appropriate ordinate scale for the different lines in the figure. Note that theory predicts $k_F + k_S > k_{AP}$ and $k_F k_S > k_{AP}/(1 + L_{AB})$. See text for further details.

al., 1997), $\langle k_P \rangle$ increases with T and decreases with [Q] (Fig. 3).

Origin of k_P polydispersity

In principle, the spread in k_p values implicitly assumed in the cumulant analysis could be explained in terms of different conformations of the guest protein or as due to an heterogeneity in the quinone concentration within the liposome population. The first hypothesis is related to the existence of several protein conformational substates, each of them having different intramolecular distances and relative orientations of the cofactors. Although several indications can be found in the literature supporting the existence of different RC substates (Kleinfeld et al., 1984b; McMahon et al., 1998; Graige et al., 1998), all the experimental evidence points to extremely short characteristic times (from 1 ps to 1 ms) (McMahon et al., 1998) for conformational interconversion at room temperature. Thus, in a time scale of seconds, the single turnover flash experiments should probe only an average protein conformation. As to the second hypothesis, from a kinetic point of view, a heterogeneity in the local UQ_{10} concentration (Q) within the liposome population should be effective on a very long time scale (hours if not days). In fact, both ubiquinone and phospholipids are practically water-insoluble species (in both cases the monomer concentration in water is beyond the detection limit of current analytical techniques); moreover, on the time scale of interest, spontaneous fusion of vesicles is extremely unlikely to occur, requiring weeks in the absence of any fusogenic agent (Sackmann, 1995).

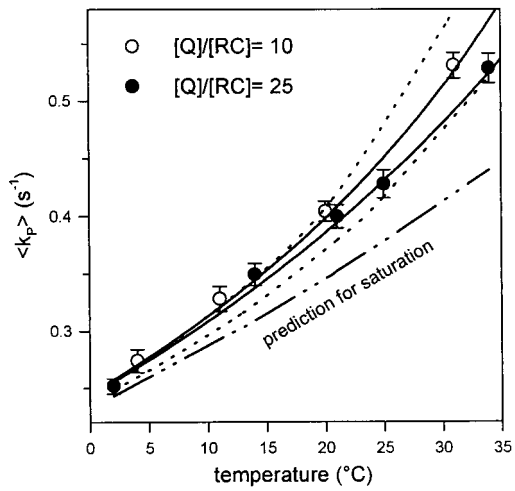

FIGURE 3 Mean rate constant, $\langle k_P \rangle$, obtained by fitting P^+ decays to Eq. 6 as a function of temperature at two different [Q]/[RC] ratios (Table 1). Dotted curves represent the predictions of Eq. 5 with $k_{AP} = 10\ s^{-1}$ and L_{AB} and K_{bind} calculated from the corresponding enthalpy and entropy changes determined in reverse micelles (Table 2). The prediction of Eq. 5 at saturating quinone concentrations is also shown (see text). Solid curves are the best fit to Eq. 5 obtained by considering simultaneously the [Q] and T dependence, with the enthalpy and entropy changes for the binding (ΔH°_{bind} and ΔS°_{bind}) and for the $Q_A^- Q_B \rightarrow Q_A Q_B^-$ (ΔH°_{AB} and ΔS°_{AB}) equilibria as adjustable parameters. The best fitting values of these parameters are listed in Table 2.

The spread in Q, in turn, can arise from two factors, namely, the random distribution of UQ_{10} molecules among vesicles and the size polydispersity of the vesicles themselves. Information on this last point has been gained by QELS analysis of the same proteoliposome preparations in which charge recombination kinetics were examined. As pointed out in Materials and Methods, if non-interacting vesicles of different size are present, each population will contribute to the decay of the autocorrelation function with a term $\exp[-D(R)q^2\tau]$, being $D(R)$ the diffusion coefficient of the population of radius R. The field autocorrelation function will be given by

$$|g_1(q, \tau)| = \int P(\Gamma) e^{-\Gamma\tau} d\Gamma \qquad (7)$$

where $P(\Gamma)$ is the appropriate normalized distribution of decay rates $\Gamma(R) = D(R)q^2$, which, for spherical particles, is related to the size distribution $P(R)$ through the Stokes-Einstein equation. The $g_2(q, \tau)$ of the samples used in charge recombination measurements were analyzed for the vesicles' mean radius and size standard deviation, using both the classical cumulant analysis (above described) and the numerical inversion of the Laplace transform represented in Eq. 7, by means of the CONTIN routine implemented by Provencher (1982). These two approaches give consistent results (Fig. 4) and show that vesicle preparations are characterized by a mean radius, $\langle R \rangle$, of 50 nm and a size standard deviation, σ_R, of about 15 nm. On this basis, the mean number of UQ_{10} molecules per vesicle can be easily evaluated once the overall quinone and lecithin number density ([Q] and [PC], respectively) are known. The total interfacial surface for unitary volume is $[PC]\alpha$, where α is the polar headgroup area of a lecithin molecule in a bilayer ($\approx 0.7\ nm^2$) (Angelico et al., 2000). Let $P(R)dR$ be the probability of finding vesicles with radii bracketed by R and $R + dR$. Neglecting the bilayer thickness, the number density of liposomes with radii lying between R and $R + dR$ is $\frac{1}{2}[PC]\alpha\ (R^2P(R)dR)/(\int R^2P(R)dR) \cdot 1/4\pi R^2$ where the term $\frac{1}{2}$ comes from the presence of two interfacial phospholipid layers per vesicle. Therefore, the total number of vesicle per unit volume, n_{lip}, is

$$n_{lip} = \int \frac{[PC]\alpha}{8\pi R^2} \frac{R^2P(R)dR}{\int R^2P(R)dR} = \frac{[PC]\alpha}{8\pi\mu_{R,2}} \qquad (8)$$

where $\mu_{R,2} = \sigma_R^2 + \langle R \rangle^2$ is the second moment of the size distribution. Thus the mean number of UQ_{10} per liposome, $\langle N \rangle$, is $[Q]/n_{lip}$.

The distribution of guest molecules among colloidal hosts has been the subject of several studies which point to a

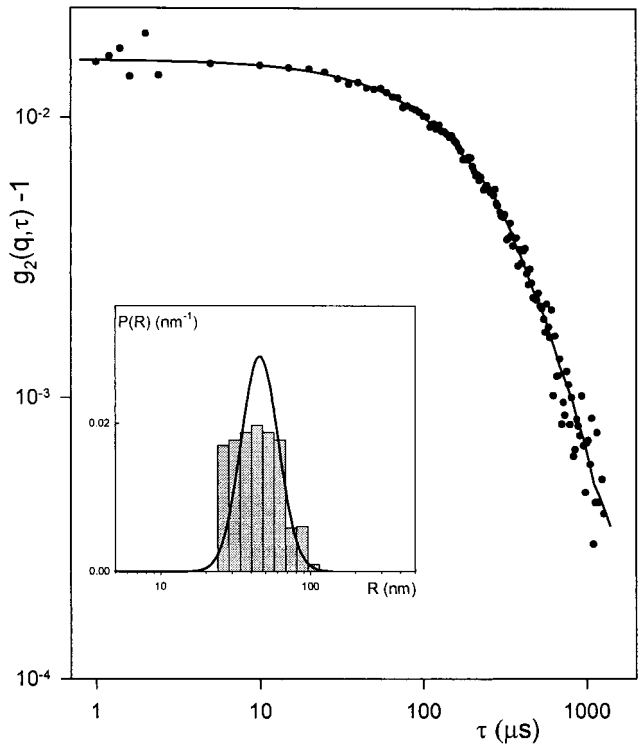

FIGURE 4 Determination of the size distribution of proteoliposomes by QELS. Log-log plot of $g_2(q, \tau) - 1$, determined in SUVs (dots) and best-fit obtained by cumulants analysis (*solid line*). The fit corresponding to the numerical inversion of the Laplace transform (CONTIN) is not shown for the sake of clarity. Experimental conditions: [Q]/[RC] = 25; T = 298 K; $\theta = 90°$; λ = 532 nm. The sample was diluted in order to minimize the intervesicle interaction. For the refractive index n and the viscosity of the solvent η_0 values of pure water have been assumed. The inset shows the size distribution obtained by CONTIN analysis (*histogram*) and the log-normal size distribution (*solid line*) characterized by the $\langle R \rangle$ and σ_R values determined by cumulant analysis of QELS data (in this case only the moments of the distribution are accessible).

Poisson distribution (Zana, 1987). Since $\langle N \rangle$ is quite high (of the order of thousands), the probability of quinone occupancy $P(N)$ can be well approximated by a Gaussian distribution function centered at $\langle N \rangle$ and with a variance $\sigma_N^2 = \langle N \rangle$. The local UQ_{10} concentration (number of molecules per unit volume of lipidic phase) into a vesicle of radius R will be $Q = N\alpha/(4\pi R^2 v_{lip})$, where the hydrophobic volume domain is calculated as the aggregation number $(4\pi R^2/\alpha)$ times the molecular volume of the lecithin hydrophobic tails (v_{lip} = 1.053 nm^3) (Angelico et al., 2000). Q is a function of N and R and can be expanded in Taylor series obtaining, at least in a first approximation, the mean value of quinone concentration $\langle Q \rangle$. This, using Eq. 8, can be written as:

$$\langle Q \rangle = \frac{\langle N \rangle \alpha}{4\pi \langle R \rangle^2 v_{lip}} = \frac{[Q]}{[PC]} \frac{2\mu_{R,2}}{v_{lip} \langle R \rangle^2} \tag{9}$$

and the variance of $P(Q)$ by means of the relationship:

$$\sigma_Q^2 = \left(\frac{\partial Q}{\partial N}\right)^2_{\substack{\langle N \rangle \\ \langle R \rangle}} \sigma_N^2 + \left(\frac{\partial Q}{\partial R}\right)^2_{\substack{\langle N \rangle \\ \langle R \rangle}} \sigma_R^2 = \left(1 + 4 \cdot \frac{\langle N \rangle \sigma_R^2}{\langle R \rangle^2}\right) \frac{\langle Q \rangle^2}{\langle N \rangle} \tag{10}$$

where the partial derivatives are evaluated at $\langle N \rangle$ and $\langle R \rangle$.

Eq. 10 deserves some comments: even in the case of monodispersed vesicles ($\sigma_R = 0$) a spread of Q with a variance $\sigma_Q^2 = \langle Q \rangle^2 / \langle N \rangle$ is expected. On the other hand, for large $\langle N \rangle$, $\sigma_Q / \langle Q \rangle = 2\sigma_R / \langle R \rangle$, which means that the degree of Q polydispersity will only depend on the vesicle size distribution and therefore any attempt to eliminate Q heterogeneity in polydispersed liposomes by increasing UQ_{10} concentration, is useless.

By means of Eqs. 9 and 10 it is thus possible to evaluate with a sufficient accuracy the first and second moments of the UQ_{10} distribution function, $P(Q)$.

$P(k_P)$, can be defined in terms of $P(Q)$ as:

$$P(k_P) dk_P = \frac{k_P P(Q) dQ}{\int k_P P(Q) dQ} \tag{11}$$

By considering that the rate constant describing the charge recombination kinetics, k_P, depends on Q according to Eq. 5, we have

$$\frac{dk_P}{dQ} = \frac{[k_{AP} - k_P(1 + L_{AB})] K_{bind}}{1 + K_{bind} Q + L_{AB} K_{bind} Q} \tag{12}$$

and, combining Eqs. 11 and 12, the rate distribution function, $P(k_P)$, can now be brought back to $P(Q)$, obtaining:

$$P(k_P) = \frac{k_{AP}(1 + K_{bind} Q)}{[k_{AP} - k_P(Q)(1 + L_{AB})] K_{bind}} \frac{P(Q)}{\int k_P P(Q) dQ} \tag{13}$$

Since both L_{AB} and K_{bind} are function of T, also $P(k_P)$ will be temperature dependent.

Rate distribution functions, $P(k_P)$, calculated over the T range investigated and for [Q]/[RC] = 25, are shown in Fig. 5. $P(k_P)$ has been evaluated assuming both a Gaussian (with a cutoff at $Q = 0$) and a log-normal distribution, $P(Q)$, of Q among vesicles. Eqs. 9 and 10 have been used to determine $\langle Q \rangle$ and σ_Q^2 from the lipid and quinone composition of the samples and from the $\langle R \rangle$ and σ_R values obtained by QELS analysis of proteoliposomes. Starting from $P(Q)$ (Fig. 5, *inset*), Eqs. 5 and 13 allow the evaluation of $P(k_P)$ at different temperatures. In these equations, L_{AB} and K_{bind} have been calculated at the appropriate temperature from the values of ΔH^o and ΔS^o for $Q_A^- Q_B \leftrightarrow Q_A Q_B^-$ electron transfer and quinone binding previously determined in reverse micelles (Mallardi et al., 1997; Table 2). The resulting $P(k_P)$ distributions, shown in Fig. 5, are compatible with the corresponding values of $\langle k_P \rangle$ determined by cumulant analysis of experimental P^+ decays (Table 1). Increasing T, $\langle k_P \rangle$ values increase and the $P(k_P)$ distribution function becomes progressively broader. Analogous simulations, in good

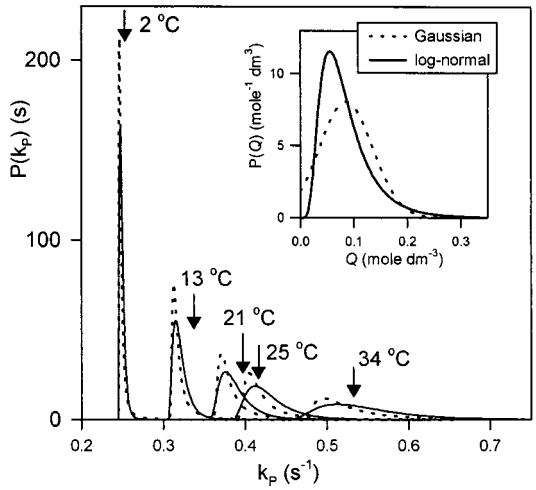

FIGURE 5 Rate distribution functions, $P(k_P)$, calculated according to Eq. 13 at different temperatures for [Q]/[RC] = 25, assuming Gaussian (*dotted*) and log-normal (*solid*) P(Q) distributions (*inset*). Values of $\langle Q \rangle$ and σ_Q^2 have been determined by means of Eqs. 9 and 10 from the lipid and quinone composition and from QELS analysis of proteoliposomes. In Eqs. 13 and 5, L_{AB} and K_{bind} have been calculated at the appropriate temperature from the corresponding enthalpy and entropy changes determined in reverse micelles (Table 2). The arrows indicate the values of $\langle k_P \rangle$ obtained from cumulant analysis of the experimental charge recombination kinetics (Table 1).

agreement with experimental $\langle k_P \rangle$ values, have been obtained at [Q]/[RC] = 10 (not shown). The predictions of Fig. 5 are relatively insensitive to the choice of the Q distribution. This last point lead us to use the first term of a Taylor expansions of $k_P(Q)$ around $\langle Q \rangle$ to evaluate $\langle k_P \rangle$ from Eq. 5 simply by posing $\langle Q \rangle = Q$. This theoretical prediction is shown in Fig. 3 (dotted line) for two values of [Q] as a function of T and is compared with the values of $\langle k_P \rangle$ coming from the cumulant analysis of the charge recombination kinetics. In Fig. 3 the T dependence expected at saturating Q, when $k_P = k_{AP}/(1 + L_{AB})$, is also presented. This prediction deviates appreciably from the theoretical behavior expected at [Q]/[RC] = 25 when the temperature increases, clearly indicating that the binding equilibrium is an important factor in determining the kinetics of charge recombination.

A comparison between simulation and experiment in the presence of 10 and 25 UQ_{10} molecules per RC molecule reveals a remarkable agreement. Indeed, the absence of any adjustable parameter in the simulations of Figs. 3 and 5 has to be emphasized: experimental points come from the cumulant analysis of the kinetic traces, while predictions were done on the basis of chemical composition of the samples, of $\langle R \rangle$ and σ_R measured by QELS, and of the thermodynamic parameter and k_{AP} values previously determined in reverse micelles. This agreement suggests that the thermodynamic parameters ruling the charge recombination kinetics are very close in SUVs and in reverse micelles. A fit of Eq. 5 performed simultaneously to the data collected at the two [Q]/[RC] ratios, under the condition $Q \equiv \langle Q \rangle$ and with the enthalpy and entropy changes for the binding (ΔH^o_{bind} and ΔS^o_{bind}) and for the $Q_A^- Q_B \rightarrow Q_A Q_B^-$ (ΔH^o_{AB} and ΔS^o_{AB}) equilibria as adjustable parameters results in a quite satisfactory description, shown in Fig. 3 by the solid lines, and yields the parameters listed in Table 2. Enthalpy and entropy changes obtained for quinone binding in reverse micelles and vesicles (Table 2) coincide within the experimental error, indicating the same quinone affinity for the Q_B binding site in SUVs and in reverse micelles. An analogous agreement is obtained between the thermodynamical parameters of $Q_A^- Q_B \rightarrow Q_A Q_B^-$ electron transfer in the two systems.

TABLE 2 Enthalpy, entropy, and free energy changes of quinone binding and $Q_A^- Q_B \rightarrow Q_A Q_B^-$ electron transfer as determined from the analysis of charge recombination kinetics in reverse micelles, phospholipid vesicles, and LDAO micelles

	Reverse micelles*	Vesicles	LDAO micelles†
	Quinone binding		
ΔH^o_{bind}/kJ mol^{-1}	-50.7 ± 3.8	-55.4 ± 3.6	
ΔS^o_{bind}/J mol^{-1}K^{-1}	-132 ± 15	-137 ± 10	
ΔG^o_{bind}/kJ mol^{-1}‡	-11.4 ± 0.9	-14.6 ± 0.6§	-9.0 ± 1.3
	$Q_A^- Q_B \rightarrow Q_A Q_B^-$ electron transfer		
ΔH^o_{AB}/kJ mol^{-1}	-13.5 ± 0.7	-15.15 ± 1.16	
ΔS^o_{AB}/J mol^{-1}K^{-1}	-19.3 ± 3.2	-25.1 ± 3.9	
ΔG^o_{AB}/kJ mol^{-1}‡	-7.7 ± 0.3	-7.67 ± 0.05§	7.8 ± 0.3

*From Mallardi et al., 1997.
†From Shinkarev and Wraight (1997).
‡Evaluated at 298 K.
§Due to the strong correlation between ΔH^o and ΔS^o, the confidence intervals for ΔG^o were evaluated by a Monte Carlo procedure as described in Mallardi et al. (1998).

Comparison with the charge recombination kinetics in detergent RC suspensions

As mentioned in the Introduction, charge recombination kinetics has been studied extensively in detergent suspensions of purple bacteria RCs. Recently, Shinkarev and Wraight (1997) have analyzed the interaction of quinone and detergent with *R. sphaeroides* RCs developing a model which allows a deep understanding of charge recombination kinetics and providing a means of determining both L_{AB} and the equilibrium constant of quinone binding at the Q_B site. In view of a comparison with the results obtained by us in phospholipid vesicles, some differences and common features which characterize the two systems investigated and the models correspondingly proposed are summarized in the following: 1) both LDAO micelles and phospholipid vesicles are disconnected lipophilic domains, but only one RC is present in each detergent micelle, together with few or none quinone molecules, whereas several RCs are inserted in the same vesicle; 2) in the detergent micelles examined by Shinkarev and Wraight (1997) the ratio [Q]/[RC] is quite low (≤ 2) while in our experiments [Q]/[RC] ≥ 10); 3) as in

vesicles, in detergent suspensions the exchange between the Q_B site and the immediate quinone pool (i.e., quinone within the same RC micelle) is assumed to be fast, while the exchange of quinone between different micelles occurs much more slowly than charge recombination. Thus (in LDAO micelles) the real physical system, established by the quinone distribution, is discrete (Shinkarev and Wraight, 1997), and the kinetics of P^+ dark relaxation is described by the sum of exponential decays (actually the deconvolution of the experimental curves was limited to two exponential components).

From a physical point of view, our approach to the vesicle system is quite similar, the main difference being due to the presence of several RC which share the same quinone-pool, i.e., our system is continuous. When this feature is coupled with the size polydispersity (high in vesicles but extremely low in RC-containing detergent micelles) and with the high [Q]/[RC] ratio allowed by vesicles, different kinetics of charge recombination naturally emerge.

Since in detergent dispersions the kinetically relevant unit is the single RC micelle containing a number n of secondary/pool quinone molecules, quinone binding affinity at the Q_B site is determined by a (dimensionless) intramicellar association constant, K_Q^+ (Shinkarev and Wraight, 1997). A comparison between the binding processes described in terms of concentrations (in vesicles and reverse micelles) and in terms of number of quinones per RC micelle (in LDAO) gives: $K_Q^+ n = K_{bind}[Q]$. We can evaluate the free energy change of quinone binding, $\Delta G^o_{bind,LDAO}$, in LDAO micelles by using the value $K_Q^+ = 0.6 \pm 0.2$ (Shinkarev and Wraight, 1997) and the relationship $\Delta G^o_{bind,LDAO} = -RT\ln(K_Q^+ N_{ag} V_{LDAO})$ where $N_{ag} = 250 \pm 50$ is the number of detergent molecules in the RC "belt" (Feher and Okamura, 1978; Gast et al., 1994) and $V_{LDAO} = 0.2557$ L mol^{-1} is the LDAO molar volume (Milioto et al., 1987). This procedure yields $\Delta G^o_{bind,LDAO} = -9.0 \pm 1.3$ kJ/mol, a value relatively close to that determined by us in phospholipid vesicles. As shown in Table 2 the free energy change of $Q_A^- Q_B \rightarrow Q_A Q_B^-$ electron transfer obtained from cumulant analysis in proteoliposomes coincides within the experimental error with that measured in LDAO RC micelles. It appears therefore that the qualitatively different kinetics of $P^+Q_B^-$ recombination observable in reverse micelles, vesicles, and LDAO direct micelles can all be brought back to the same process (governed by very similar thermodynamical parameters in the different environments), i.e., the fast exchange of quinone molecules between the protein binding site and a quinone pool. The hosting systems only defines the boundary conditions: number of RC sharing the same pool, size of the pool, heterogeneity of the lipophilic domain size, and rate of exchange between quinone pools in different domains.

CONCLUSION

A new approach, based on the formalism of the statistical cumulant generating function, has been developed to analyze the kinetics of charge recombination in RCs incorporated into small unilamellar phospholipid vesicles containing a large ubiquinone pool. This analysis, when considering the distribution of UQ_{10} molecules in the vesicle population and the size polydispersity of proteoliposomes probed by QELS measurements, accounts satisfactorily for the non-exponential kinetics of $P^+Q_B^-$ recombination observed over a range of temperatures at different [Q]/[RC] ratios. The model provides a means of determining the equilibrium constant of quinone binding at the Q_B site and of electron transfer between Q_A and Q_B in a lipid environment mimicking the native membrane. The proposed approach provides a starting point in the analysis of the interaction between small lipophilic cofactors and membrane enzymes directly into the lipid matrix.

We are indebted to Dr. L. Ambrosone for valuable suggestions and wish to thank Prof. B. Andrea Melandri for critically reading the manuscript. The financial support of MURST of Italy is acknowledged by G.P. (PRIN 1997 Struttura Proprietà e Dinamica di Sistemi di Interesse Biologico) and G.V. (PRIN 1997, Bioenergetica e Trasporto di Membrana). G.P., A.M., and M.G. dedicate this work to the memory of their friend and colleague professor Americo Inglese.

REFERENCES

Agostiano, A., L. Catucci, M. Della Monica, A. Mallardi, G. Palazzo, and G. Venturoli. 1995. Charge recombination kinetics of photosynthetic reaction centers in water-in-oil phospholipid organogels. *Bioelectrochem. Bioenerg.* 38:25–33.

Allen, J. P., G. Feher, T. O. Yeates, H. Komiya, and D. C. Rees. 1987a. Structure of the reaction center from *Rhodobacter sphaeroides* R-26: the cofactors. *Proc. Natl. Acad. Sci. USA.* 84:5730–5734.

Allen, J. P., G. Feher, T. O. Yeates, H. Komiya, and D. C. Rees. 1987b. Structure of the reaction center from *Rhodobacter sphaeroides* R-26: the protein subunits. *Proc. Natl. Acad. Sci. USA.* 84:6162–6166.

Angelico, R., A. Ceglie, U. Olsson, and G. Palazzo. 2000. Phase diagram and phase properties of the system lecithin-water-cyclohexane. *Langmuir.* 16:2124–2132.

Baciou, L., E. Rivas, and P. Sebban. 1990. $P^+Q_A^-$ and $P^+Q_B^-$ charge recombinations in *Rhodopseudomonas viridis* chromatophores and in reaction centers reconstituted in phosphatydilcholine liposomes: existence of two conformational states of the reaction centers and effects of pH and of o-phenanthroline. *Biochemistry.* 29:2966–2976.

Beechem, J. M. 1992. Global analysis of biochemical and biophysical data. *Methods Enzymol.* 210:37–54.

Berti, D., P. Barbaro, I. Bucci, and P. Baglioni. 1999. Molecular recognition through H-bonding in micelles formed by dioctylphosphatidyl nucleosides. *J. Phys. Chem. B.* 103:4916–4922.

Chu, B. 1991. Laser Light Scattering: Basic Principles and Practice, Second Edition. Academic Press, New York.

Corti, M. 1985. The laser light scattering technique and its application to micellar solutions. *In* Physics of Amphiphiles, Micelles, Vesicles and Microemulsions, Proceedings of the International School of Physics "Enrico Fermi," M. Corti and V. Degiorgio, editors. North-Holland Physics Publishing, Amsterdam. 122–151.

Cramer, W. A., and D. B. Knaff. 1990. *Energy Transduction in Biological Membranes.* Springer-Verlag, New York.

Crofts, A. R., and C. A. Wraight. 1983. The electrochemical domain of photosynthesis. *Biochim. Biophys. Acta.* 726:149–185.

Deisenhofer, J., O. Epp, K. Miki, R. Huber, and H. Michel. 1984. X-ray structure analysis of a membrane protein complex: electron density map at 3Å resolution and a model of the chromophores of the photosynthetic

reaction center from *Rhodopseudomonas viridis. J. Mol. Biol.* 180: 385–398.

Deisenhofer, J., O. Epp, K. Miki, R. Huber, and H. Michel. 1985. Structure of the protein subunits in the photosynthetic reaction centers of *Rhodopseudomonas viridis* at 3Å resolution. *Nature.* 318:618–624.

Ermler, U., G. Fritzsch, S. K. Buchanan, and H. Michel. 1994. Structure of the photosynthetic reaction centre from Rhodobacter sphaeroides at 2.65Å resolution: cofactors and protein-cofactor interactions. *Structure.* 2:925–936.

Feher, G., J. P. Allen, M. Y. Okamura, and D. C. Rees. 1989. Structure and function of bacterial photosynthetic reaction centres. *Nature.* 33: 111–116.

Feher, G., T. R. Arno, and M. Y. Okamura. 1988. The effect of an electric field on the charge recombination rate of $D^+Q_A^- \rightarrow DQ_A$ in reaction centers from *Rhodobacter sphaeroides* R-26. *In* The Photosynthetic Bacterial Reaction Center. J. Breton and A. Vermeglio, Editors. Plenum, New York. 271–287.

Feher, G., and M. Y. Okamura. 1978. Chemical composition and properties of reaction centers. *In* The Photosynthetic Bacteria. R. K. Clayton and W. R. Sistrom, Editors. Plenum Press, New York. 349–386.

Feher, G., M. Okamura, and D. Kleinfeld. 1987. Electron transfer reactions in bacterial photosynthesis: charge recombination kinetics as a structure probe. *In* Protein Structure: Molecular and Electronic Reactivity. R. Austin, E. Buhks, B. Chance, D. De Vault, P. L. Dutton, H. Frauenfelder, and V. I. Gol'danskii, Editors. Springer-Verlag, New York. 399–421.

Gao, J-L., R. J. Shopes, and C. A. Wraight. 1991. Heterogeneity of kinetics and electron transfer equilibria in the bacteriopheophytin and quinone electron acceptors of reaction centers from *Rhodopseudomonas viridis. Biochim. Biophys. Acta.* 1056:259–272.

Gast, P., P. Hemerlijk, and A. J. Hoff. 1994. Determination of the number of detergent molecules associated with the reaction center protein isolated from the photosynthetic bacterium *Rodopseudomonas viridis.* Effects of the amphiphilic molecule 1,2,3-heptantriol. *FEBS Lett.* 337:39–42.

Graige, M. S., G. Feher, and M. Y. Okamura. 1998. Conformational gating of the electron transfer reaction $Q_A^- Q_B \rightarrow Q_A Q_B^-$ in bacterial reaction centers of *Rhodobacter sphaeroides* determined by a driving force assay. *Proc. Natl. Acad. Sci. USA.* 95:11679–11684.

Gray, K. A., J. Wachtveitl, J. Breton, and D. Oesterhelt. 1990. Initial characterization of site-directed mutants of tyrosine M210 in the reaction centre of *Rhodobacter sphaeroides. EMBO J.* 9:2061–2070.

Gunner, M. R. 1991. The reaction center protein from purple bacteria: structure and function. *Curr. Topics Bioenerg.* 16:319–367.

Gunner, M. R., A. Nicholls, and B. Honig. 1996. Electrostatic potentials in *Rhodopseudomonas viridis* reaction centres: implications for the driving force and directionality of electron transfer. *J. Phys. Chem.* 100:4277–4291.

Gunner, M. R., D. E. Robertson, and P. L. Dutton. 1986. Kinetic studies on the reaction center protein from *Rhodopseudomonas sphaeroides:* the temperature and free energy dependence of electron transfer between various quinones in the Q_A site and the oxidized bacteriochlorophyll dimer. *J. Phys. Chem.* 90:3783–3795.

Kleinfeld, D., M. Y. Okamura, and G. Feher. 1984a. Electron transfer in reaction centers of *Rhodopseudomonas sphaeroides.* I. Determination of the charge recombination pathway of $D^+Q_AQ_B^-$ and free energy and kinetic relations between $Q_A^-Q_B$ and $Q_AQ_B^-$. *Biochim. Biophys. Acta.* 766:126–140.

Kleinfeld, D., M. Y. Okamura, and G. Feher. 1984b. Electron transfer kinetics in photosynthetic reaction centers cooled to cryogenic temperatures in the charge-separated state: evidence for light-induced structural changes. *Biochemistry.* 23:5780–5786.

Kleinfeld, D., M. Y. Okamura, and G. Feher. 1985. Electron transfer in reaction centers of *Rhodopseudomonas sphaeroides.* II. Free energy and kinetic relations between the acceptor states $Q_A^-Q_B^-$ and $Q_AQ_B^{2-}$. *Biochim. Biophys. Acta.* 809:291–310.

Koppel, D. E. 1972. Analysis of macromolecular polydispersity in intensity correlation spectroscopy: the method of cumulant. *J. Chem. Phys.* 57: 4814–4820.

Labahn, A., J. M. Bruce, M. Y. Okamura, and G. Feher. 1995. Direct charge recombination from $D^+Q_AQ_B^-$ to DQ_AQ_B in bacterial reaction centers from *Rhodobacter sphaeroides* containing low potential quinone in the Q_A site. *Chem. Phys.* 197:355–366.

Nagy, L., E. Fodor, J. Tandori, L. Rinyu, and T. Farkas. 1999. Lipids affect the charge stabilization in wild-type and mutant reaction centers of *Rhodobacter sphaeroides* R-26. *Aust. J. Plant Physiol.* 26:465–473.

Mallardi, A., M. Giustini, and G. Palazzo. 1998. Binding of ubiquinone to photosynthetic reaction centers. 2. Determination of enthalpy and entropy changes for the binding to the QA site in reverse micelles. *J. Phys. Chem. B.* 102:9168–9173.

Mallardi, A., G. Palazzo, and G. Venturoli. 1997. Binding of ubiquinone to photosynthetic reaction centers: determination of enthalpy and entropy changes in reverse micelles. *J. Phys. Chem. B.* 101:7850–7857.

Mancino, J., D. P. Dean, and R. E. Blankenship. 1984. Kinetics and thermodynamics of the $P870^+Q_B^-$ reaction in isolated reaction centers from the photosynthetic bacterium *Rhodopseudomonas sphaeroides. Biochim. Biophys. Acta.* 764:46–54.

McMahon, B. H., J. D. Müller, C. A. Wraight, and G. U. Nienhaus. 1998. Electron transfer and protein dynamics in the photosynthetic reaction center. *Biophys. J.* 74:2567–2587.

McPherson, P. H., M. Y. Okamura, and G. Feher. 1990. Electron transfer from the reaction center of *Rb. sphaeroides* to the quinone pool: doubly reduced Q_B leaves the reaction center. *Biochim. Biophys. Acta.* 1016:289–292.

Milioto, S., D. Romancini, and R. De Lisi. 1987. Excess enthalpies of solution of primary and secondary alcohols in dodecyldimethylamine oxide micellar solutions. *J. Solution Chem.* 16:943–956.

Ortega, J. M., P. Mathis, J. C. Williams, and J. P. Allen. 1996. Temperature dependence of the reorganization energy for charge recombination in the reaction center from Rhodobacter sphaeroides. *Biochemistry.* 35: 3354–3361.

Provencher, S. W. 1982. A constrained regularization method for inverting data represented by linear algebraic or integral equations. *Comp. Phys. Comm.* 27:213–227.

Sackmann, E. 1995. Physics of vesicles. *In* Structure and Dynamics of Membranes, Vol. 1. R. Lipowsky and E. Sackmann, Editors. Elsevier, Amsterdam. 213–304.

Shinkarev, V. P., and C. A. Wraight. 1993. Electron and proton transfer in the acceptor quinone complex of reaction centers of phototrophic bacteria. *In* The Photosynthetic Reaction Center, Vol. 1. J. Deisenhofer and J. R. Norris, Editors. Academic Press, New York. 193–245.

Shinkarev, V. P., and C. A. Wraight. 1997. The interaction of quinone and detergent with reaction centers of purple bacteria. I. Slow quinone exchange between reaction center micelles and pure detergent micelles. *Biophys. J.* 72:2304–2319.

Stowell, M. H. B., T. M. McPhillips, D. C. Rees, S. M. Soltis, E. Abresch, and G. Feher. 1997. Light-induced structural changes in photosynthetic reaction center: implications for mechanism of electron-proton transfer. *Science.* 276:812–816.

Venturoli, G., A. Mallardi, and P. Mathis. 1993. Electron transfer from cytocrome c_2 to the primary donor of *Rhodobacter sphaeroides* reaction centers: a temperature dependence study. *Biochemistry.* 32: 13245–13253.

Vermeglio, A., and R. K. Clayton. 1977. Kinetics of electron transfer between the primary and the secondary electron acceptors in reaction center from *Rhodopseudomonas sphaeroides. Biochim. Biophys. Acta.* 461:159–165.

Wraight, C. A. 1981. Oxidation-reduction physical chemistry of the acceptor quinone complex in bacterial photosynthetic reaction centers: evidence for a new model of herbicide activity. *Israel. J. Chem.* 21: 348–354.

Zana, R. 1987. Luminescent probing methods. *In* Surfactant Solutions: New Methods of Investigation. R. Zana, Editor. Marcel Dekker, New York. 241–294.